



Seismic evidence for an Iceland thermo-chemical plume in the Earth's lowermost mantle



Yumei He^{a,*}, Lianxing Wen^{b,c}, Yann Capdeville^d, Liang Zhao^e

^a Key Laboratory of Earth and Planetary Physics, Institute of Geology and Geophysics, Chinese Academy of Sciences, Beijing 100029, PR China

^b Department of Geosciences, State University of New York at Stony Brook, Stony Brook, NY 11790, USA

^c Laboratory of Seismology and Physics of Earth's Interior, University of Science and Technology of China, Hefei, Anhui, 230026, PR China

^d Institut de Physique du globe de Paris, 4, place Jussieu, Paris, 75005, France

^e State Key Laboratory of Lithospheric Evolution, Institute of Geology and Geophysics, Chinese Academy of Sciences, Beijing 100029, PR China

ARTICLE INFO

Article history:

Received 5 November 2014

Received in revised form 13 February 2015

Accepted 14 February 2015

Available online xxxxx

Editor: P. Shearer

Keywords:

mantle plume

Iceland

shear wave velocity structure

lowermost mantle

ABSTRACT

We constrain the geographic extent, geometry and velocity structure of the seismic anomaly near the Earth's core–mantle boundary (CMB) beneath Iceland, based on travel time and three-dimensional waveform modeling of the seismic data sampling the lowermost mantle beneath Iceland. Our analysis suggests a mushroom-shaped low velocity anomaly situated in the lowermost mantle beneath Iceland surrounded by a high velocity province. The best fitting mushroom-shaped model is 600 km high and has a stem with a radius of 350 km in the lowermost 250 km of the mantle and a cap with increasing radii from 550 km at 250 km above the CMB to 650 km at 600 km above the CMB. The shear velocity structure varies from 0% at the top to –3% at 250 km above the CMB and to –6% at the CMB. These inferred seismic features, in combination with the previous evidence of existence of ultra-low velocity zones at the base of the mantle beneath the region, suggest that Iceland represents a thermo-chemical plume generated by interaction of downwelling and a localized chemical anomaly at the base of the mantle.

© 2015 Elsevier B.V. All rights reserved.

1. Introduction

Iceland is characterized by an anomalously thick crust (Foulger et al., 2003), a major, strong, low-wave-speed anomaly in the upper mantle (Tryggvason et al., 1983; Wolfe et al., 1997; Bijwaard and Spakman, 1999; Ritsema et al., 1999; Zhao, 2001; Hung et al., 2004; Montelli et al., 2006), local thinning of the transition zone (Shen et al., 1998), atypical geochemical signatures (Farley and Neroda, 1998; Mukhopadhyay, 2012), and has long been proposed as the manifestation of a mantle plume rising from the core–mantle boundary (CMB) (Morgan, 1971). While there has been accumulated evidence for a mantle plume in the upper mantle and the transition zone, the direct evidence for a seismic anomaly in the lowermost mantle has been limited to just the presence of ultra-low velocity zone in the region (Helmlberger et al., 1998). The detailed geometry and velocity structure of the Iceland anomaly near the CMB remain largely unconstrained, fueling

the debate of its plume origin from deep mantle (Foulger, 2002; Depaolo and Manga, 2003; Montelli et al., 2006; Mukhopadhyay, 2012; Anderson and Natland, 2014).

In this study, we are able to constrain the detailed seismic features of the lowermost mantle beneath Iceland, based on differential time residuals analysis and three-dimensional (3-D) seismic waveform modeling of the seismic data. The seismic results not only provide evidence to support the hypothesis that the Iceland is a mantle plume erupted from the core–mantle boundary, but also reveal thermo-chemical origin of the plume and likely formation mechanism of the plume. We present seismic data in Section 2, differential time residuals analysis and seismic modeling results in Section 3, and possible origin of the Iceland anomaly in Section 4.

2. Seismic data

Seismic data are collected from the database of the Incorporated Research Institutions for Seismology (IRIS). A Butterworth filter with a frequency range of 0.008–1 Hz is applied to all seismograms in the travel time analysis. We measure ScS–S and sScS–sS differential travel times by the difference of peak-to-peak times of the two phases on the transverse components of seismograms.

* Corresponding author.

E-mail address: ymhe@mail.igcas.ac.cn (Y. He).

Table 1
Events for travel time analysis.

Origin time	mb	Latitude (°N)	Longitude (°E)	Depth (km)
1999.316.16.57.20	6.3	40.76	31.16	10
2004.149.12.38.44	6.2	36.25	51.62	17
2004.301.20.34.37 ^a	5.8	45.79	26.62	96
2006.169.18.28.02	5.5	33.03	−39.70	10
2008.006.05.14.20 ^a	6.1	37.22	22.69	75
2009.188.19.11.47	5.9	75.35	−72.45	19
2009.250.22.41.37	5.7	42.66	43.44	15
2010.067.02.32.34	5.9	38.87	39.98	12
2010.101.22.08.13	6.0	36.97	−3.54	610

^a sScS–sS differential travel time residuals are used.

We further use waveforms of events (2002/03/03 and 2003/12/26) recorded in the United States National Seismic Network, the Canadian National Seismograph Network, the Lamont–Doherty Cooperative Seismographic Network, the Global Seismograph Network (GSN), the Cooperative New Madrid Seismic Network and the GEO-FON to constrain the detailed geometric feature and seismic structures of the Iceland anomaly in the lowermost mantle (Fig. 2). The waveforms are deconvolved with their instrumental responses and bandpass-filtered from 0.008 to 0.125 Hz.

3. Geographic boundary and shear-velocity structure of the Iceland anomaly in the lowermost mantle

3.1. Geographic boundary of the Iceland anomaly near the CMB

We first constrain the geographic extent of the Iceland anomaly near the CMB using ScS–S and sScS–sS differential travel-time residuals. We examine broadband tangential displacements of ScSH–SH and sScS–sS phases recorded at a distance range between 45° and 85° for all the events occurring from 1999 to 2010, with a magnitude greater than 5.5 and their ScS and sScS bouncing points at the CMB located between 45°–80°N and −60°–36°E. We choose 9 earthquakes and hand-pick a total of 54 ScS–S and 17 sScS–sS travel-time residuals (Table 1). The seismic data provide good coverage in our study area (Fig. 1(a)). We test six tomographic models: GyPSuM (Simmons et al., 2010), HMSL_S06 (Houser et al., 2008), S362ANI (Kustowski et al., 2008), S40RTS (Ritsema et al., 2011), SAW642ANB (Panning et al., 2010) and TX2011 (Grand, 2002) in the corrections for the effects of the seismic heterogeneities 500 km above the CMB. We choose model S362ANI (Kustowski et al., 2008) for corrections as that model produces the best correction between the corrected ScS travel time residuals and the corrected ScS–S differential travel time residuals, and removes the anti-correlation between the observed S travel time residuals and the observed ScS–S differential travel time residuals at most (Table 2). Average velocity perturbations of lowermost 500 km of the mantle beneath Iceland are estimated based on the corrected ScS–S and sScS–sS differential travel time residuals. The corrected ScS–S and sScS–sS differential travel time residuals exhibit an approximately circular area of positive values (low velocities) with radius of ~400 km beneath Iceland surrounded by regions with normal or negative values (high velocities) (Fig. 1(b)).

3.2. Geometric feature and velocity structure of the Iceland anomaly

To further constrain the geometric feature and velocity structure of the low-velocity anomaly beneath Iceland, we select seismic data from events 2002/03/03 and 2003/12/26 with their ray paths sampling inside and outside the anomaly for waveform modeling (Fig. 2(a) and Table 3). Event 2002/03/03 occurred in the Hindu Kush region and was recorded in North America. The tangential displacements of the event gradually vary with azimuth,

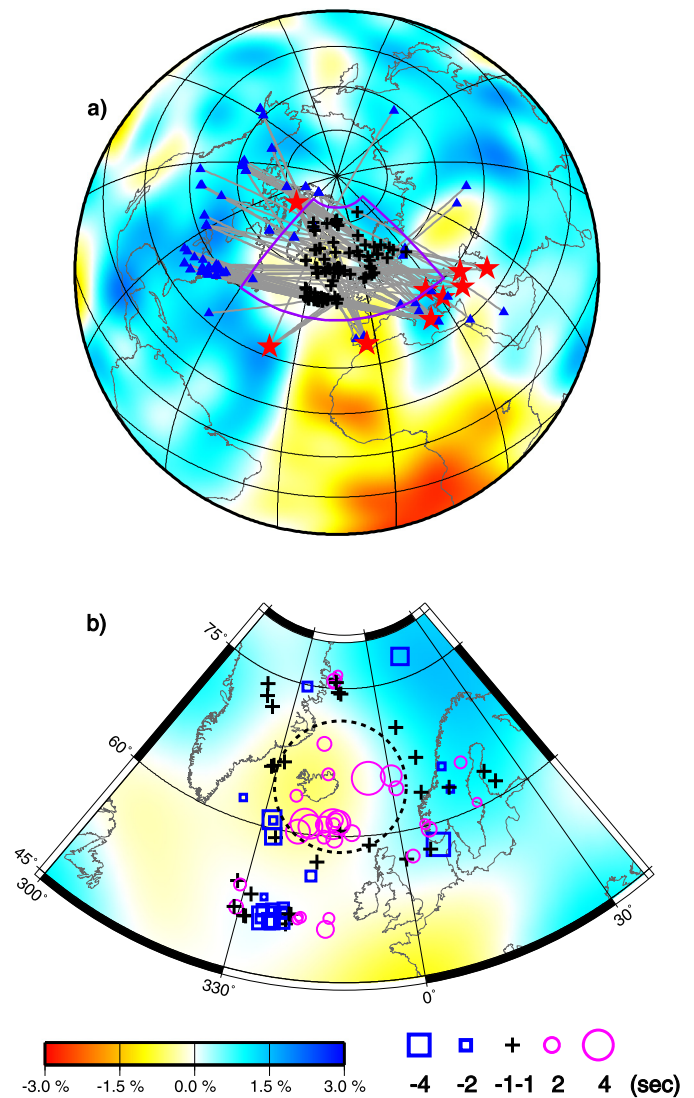


Fig. 1. (a) The study region and ScS, sScS reflected points (black crosses) at the CMB, along with earthquakes (red stars), seismic stations (deep blue triangles) and great-circle paths (gray lines) of the seismic phases used in this study. The background is shear-velocity perturbations from a global shear-velocity tomographic model S362ANI (Kustowski et al., 2008). (b) Observed ScS–S and sScS–sS differential travel time residuals plotted at the ScS and sScS reflected points at the CMB, after corrected for the effects of the mantle heterogeneities 500 km above the CMB using a shear-velocity model S362ANI (Kustowski et al., 2008). The residuals smaller than −1 s are plotted as blue squares; those ranging from −1 to 1 s as black crosses; and those larger than 1 s as purple circles. The sizes of the symbols are proportional to the magnitudes of the travel-time residuals. The boundary from positive travel-time residuals (low velocities) to zero or negative travel-time residuals (neutral or high velocities) is mapped out approximately by a dashed circle. (For interpretation of the references to color in this figure legend, the reader is referred to the web version of this article.)

Table 2
Correlation Coefficients (CC).

	CC between S and ScS–S	CC between ScS and ScS–S
Raw data	−0.16	0.61
GyPSuM	−0.30	0.53
HMSL_S06	−0.42	0.33
S362ANI	−0.04	0.65
S40RTS	−0.33	0.58
SAW642ANB	−0.20	0.58
TX2011	−0.30	0.51

from sampling the northern portion of the anomaly to outside the anomaly. Event 2003/12/26 occurred in southern Iran and was

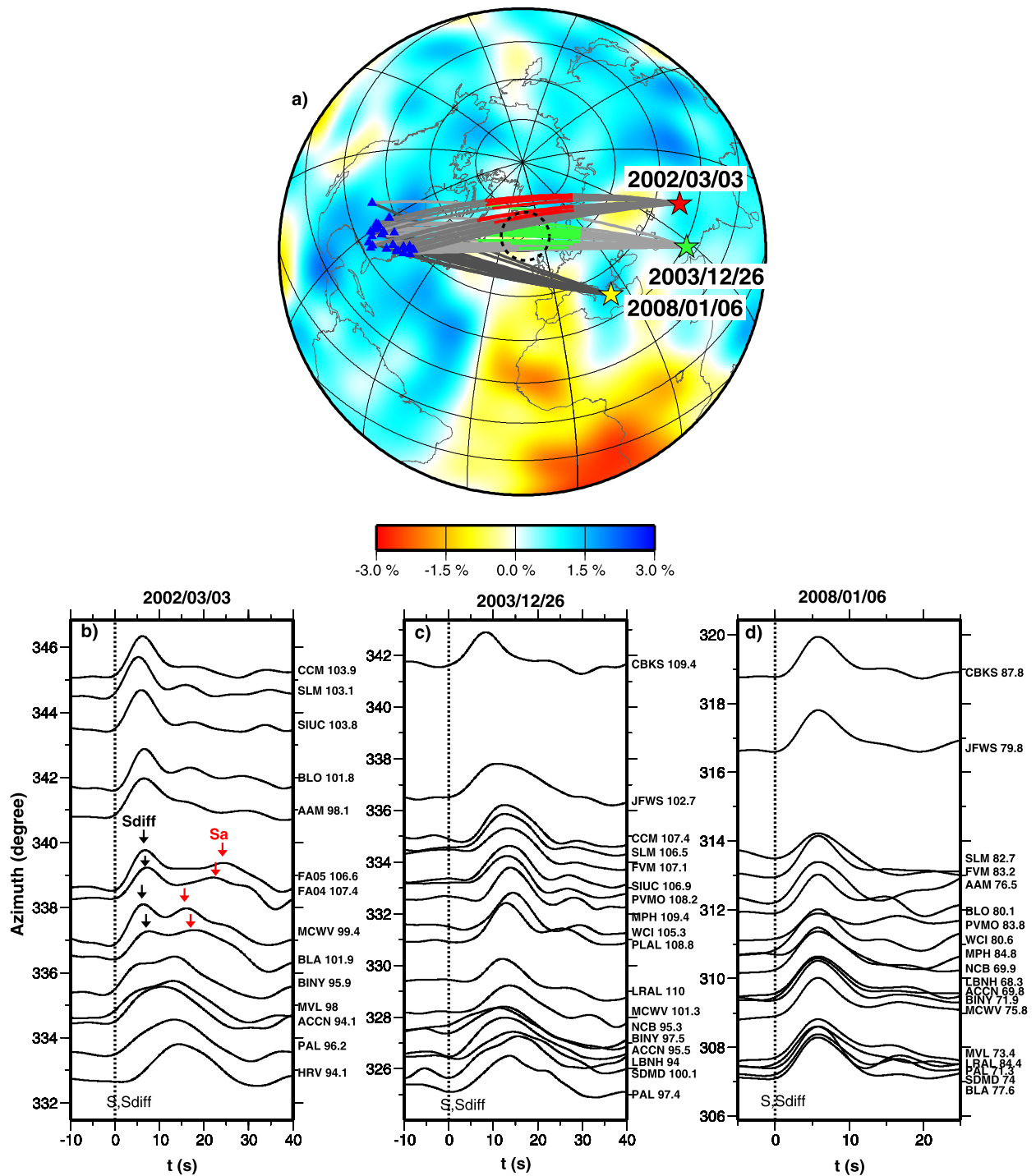


Fig. 2. (a) Geometry of events and stations used for waveform modeling. S, Sdiff raypaths in the lowermost 100 km of the mantle (red and green bold lines), along with earthquakes (red, green and yellow stars), seismic stations (deep blue triangles) and great-circle paths (gray lines), for earthquakes 2002/03/03, 2003/12/26 and 2008/01/06 whose waveforms are used to constrain the detailed geometry and seismic structures of the Iceland Anomaly in the lowermost mantle (Supplementary Fig. 1). Tomographic shear velocity perturbations at the CMB are also plotted as background (Kustowski et al., 2008). (b) Observed tangential displacements as a function of azimuth for event 2002/03/03. (c) Observed tangential displacements as a function of azimuth for event 2003/12/26. (d) Observed tangential displacements as a function of azimuth for event 2008/01/06. In Figs. 2(b)–2(d), the name and epicentral distance of each station are indicated on the right. The theoretical arrivals of S, Sdiff phases based on PREM (Dziewonski and Anderson, 1981) are plotted in dashed lines in Figs. 2(b)–2(d), and the observed S, Sdiff and S_a phases are indicated by black and red arrows in Fig. 2(b), respectively. (For interpretation of the references to color in this figure legend, the reader is referred to the web version of this article.)

recorded in North America. Its ray paths of S, Sdiff phase sample the interior of the anomaly. The seismic data of these two events sample inside and outside the anomaly, placing tight constraints on the geometry and velocity structure of the anomaly, as well as the detailed transitional structure from the anomaly to the surrounding mantle.

Travel time correction for the seismic data from events 2002/03/03 and 2003/12/26 consists of two procedures: 1. We re-determine location and origin time of the chosen earthquakes using seismic observations recorded by the GSN, a global crustal model CRUST 2.0 (Bassin et al., 2000) and a 3-D shear velocity tomographic model S362ANI (Table 2; Kustowski et al., 2008). 2. We correct

Table 3
Events list.

Event	mb	Origin time	Latitude (°N)	Longitude (°E)	Depth (km)	Time corr. (s)
2002/03/03	6.3	2002.062.12.08.20	36.50(36.50)	70.48(70.63)	226(214)	−2.0
2003/12/26	6.0	2003.360.01.56.52	29.00(29.00)	58.31(58.21)	10(4)	1.0
2008/01/06 ^a	6.1	2008.006.05.14.20	37.22(37.22)	22.69(23.09)	75(79)	−2.5

Values in parentheses are relocated latitude, longitude and depth.

^a Earthquake used as reference event for the additional correction for the SH data.

for the travel-time residuals that are caused by the seismic heterogeneities 500 km above the CMB. The corrections consist of travel-time residuals predicted on the basis of the global crustal model and shear velocity tomographic model and an additional component associated with the underestimation of the global crustal model and shear velocity tomographic model (Table 3 and Supplementary Fig. 1). The corrected travel-time residuals are attributed to the Iceland Anomaly.

The waveform complexities of event 2002/03/03 vary mainly with increasing azimuth at the distance range of 94°–107° (Fig. 2(b)). For example, seismic waveforms at stations MVL and BINY with similar azimuths exhibit similar characteristics although they have different epicentral distances of 98° and 95.9°. The widths of SH phases gradually increase and the travel time delays decrease in an azimuthal range from 333° to 335.7°. Seismic waves exhibit a clear SH phase at small azimuths followed by an anomalous phase (labeled S_a) in an azimuthal range from 336° to 339°, then back to a simple SH phase at large azimuths up to 345°. The anomalous phase exhibits same polarity and comparable amplitude as the direct SH phase and its separation from the direct S phase varies from 10 s at 336° to ~17 s at 339°. The waveform complexities are most likely caused by the laterally varying seismic heterogeneities in the lowermost mantle, as they cannot be explained by other factors, such as mislocation of the earthquake, complex source time function and the seismic heterogeneities in the source-side mantle. The data section has an azimuthal range of 333°–345°, and their ray paths are close near the source and in the source-side mantle. Mislocation of the earthquake or a complex source or the seismic heterogeneities in the source-side mantle would produce similar waveform complexities across the record section, different from the observations (Fig. 2(b)). Near-station effects and the upper mantle structure beneath North America also contribute little to the waveform complexities, because the records at the same stations for one event 2008/01/06 occurring in southern Greece, which have similar ray paths in the receiver side mantle as the data from event 2002/03/03, show simple waveforms (Figs. 2(a) and 2(d)). Moreover, the SKS phases of event 2002/03/03 show simple and similar waveforms across the stations (Supplementary Fig. 2). The above observations rule out the possibility of contributions of receiver-side crust and upper mantle heterogeneities as the cause of the observed waveform complexities of the Sdiff phases for event 2002/03/03.

The ray paths of SH, Sdiff phases for event 2003/12/16 sample the interior of the anomaly from south to north (Fig. 2(a)). The travel time and waveform of the event vary mainly with sampling azimuth at the distance range of 94°–110° (Fig. 2(c)). The SH phases exhibit travel-time delays gradually increasing from 0 s at an azimuth of 325° to 6 s at 333° and then decreasing to 0 s at ~337°. The width of the SH phase waveform decreases from 31 s at 325° to 16 s at around 333°, and gradually increases to 29 s at 337°. Based on the same arguments for event 2002/03/03, we can infer that the systematical travel-time delays and anomalous waveforms are most likely caused by the laterally varying seismic heterogeneities in the lowermost mantle beneath Iceland.

We constrain the geometric and velocity features of the anomaly in the lowermost mantle beneath Iceland through 3-D waveform

modeling of the seismic data recorded for events 2002/03/03 and 2003/12/26. We apply a coupled normal mode/spectral element method to calculate synthetic seismograms (Capdeville et al., 2003), with source mechanism obtained from the Harvard centroid moment tensor catalog (Dziewonski et al., 1981). The corrected ScS–S and sScS–sS differential travel time residuals reveal that the low velocity anomaly has a maximum radius of ~400 km near the CMB. With this constraint, we test models of a low-velocity anomaly at the base of mantle with four different shapes (mushroom, inverse dome, cylinder and cone) surrounded by a high velocity structure (Fig. 3). The radius and velocity structure of the lowermost portion of the anomaly are constrained by the observed travel time delays and anomalous waveforms of Sdiff phases of event 2003/12/26. The preferred models for the lowermost portion of the anomaly have a radius of 350 km (for models with shapes of mushroom, inverse dome or cylinder) or 400 km (for the cone-shaped model) and velocity reductions from −3% at 250 km above the CMB to −6% at the CMB. The synthetics of such models match the observations of event 2003/12/26 well (Fig. 3, bottom panel). While models with a radius smaller than 300 km and larger velocity reductions (for example, from −4% at 250 km to −7% at CMB) could produce Sdiff phase travel time delays similar to the observations, they would generate a secondary phase at station JFWS that mismatch the observed Sdiff waveform. The preferred models of the lowermost 250 km of the anomaly constrained by the seismic data of event 2003/12/26 also generate a secondary phase (labeled as S_{3d}) at stations FA04 and FA05 for event 2002/03/03 matching the observations (Fig. 3, middle panel and Fig. 4, bottom panel). In this sampling geometry, the direct Sdiff phase is generated by the seismic structure outside the low-velocity anomaly, while the secondary phase by the velocity structure inside the low-velocity anomaly. However, models of cylinder or cone shape cannot produce a secondary phase (labeled as S_{2d}) as those observed at stations BLA and MCWV (Fig. 3, middle panel), as seismic waves to these stations now sample outside the low-velocity anomaly. A secondary phase at stations BLA and MCWV can only be generated in the models with mushroom or inverse dome shapes. In those models, the waveform complexities are reproduced with S, Sdiff phases propagating the bottom high velocity structure and the secondary phases sampling the upper low velocity that overlies the high-velocity structure (Fig. 5). In another word, the waveform complexities observed at stations BLA and MCWV can only be explained when the geographic extent of the low-velocity anomaly in 250 km above the CMB is larger than that in the bottom 250 km of the mantle and when a high-velocity structure is present in the lowermost 250 km of the mantle. We prefer the mushroom-shaped model since the synthetics produced by this model fit the observations slightly better than those of the inverse dome-shaped model (Fig. 3). The observed waveform complexities place constraints on the lateral dimension of the cap in the mushroom-shaped models. A cap with a radius smaller than 500 km would not produce a strong secondary phase at stations BLA and MCWV, and the cap with a radius greater than 700 km would produce an extra secondary phase at stations FA04 and FA05 different from the observations. We have no tight constraints on the thickness of the model. However, the travel time delay of SH phase observed

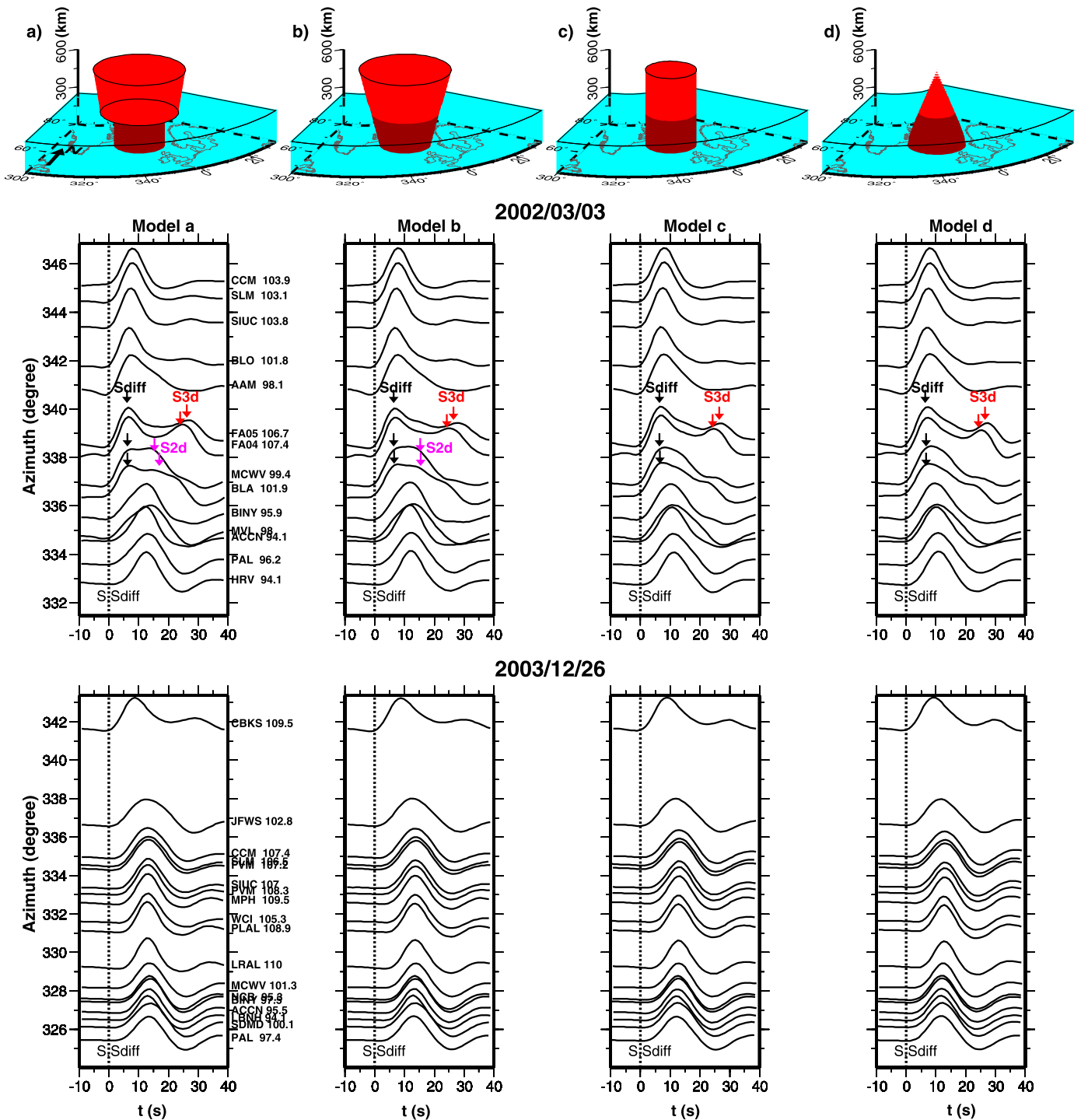


Fig. 3. Four tested models and synthetics. Top panel: Four kinds of models tested in our forward modeling process. (a) Mushroom-shaped model. It has a cap with increasing radii from 550 km at the bottom to 650 km at the top, a stem with a radius of 350 km. (b) Inverse dome-shaped model. The radius gradually varies from 650 km at the top to 350 km at the CMB. (c) Cylinder-shaped model. It has a radius of 350 km. (d) Cone-shaped model with a radius of 400 km at the CMB. All models have a total thickness of 600 km. The velocity structures vary for 0% at the top to -3% at 250 km above the CMB, and to -6% at the CMB. The surrounding high velocity structure is shown in green. Middle panel from left to right: Synthetics for event 2002/03/03 calculated based on the 3D models (a), (b), (c) and (d) illustrated in the top panel. The S , S_{diff} , S_{2d} and S_{3d} phases are indicated by black, purple and red arrows in the synthetics. Bottom panel from left to right: Synthetics for event 2003/12/26 calculated based on the 3D models (a), (b), (c) and (d) illustrated in the top panel. (For interpretation of the references to color in this figure legend, the reader is referred to the web version of this article.)

at station HRV suggests that the thickness of anomaly is greater than 500 km. The best fitting mushroom-shaped model for the low-velocity anomaly is 600 km high and has a stem with a radius of 350 km in the lowermost 250 km at the mantle and a cap with increasing radii from 550 km at the 250 km above the CMB to 650 km at the top (Fig. 3(a)). The velocity structure varies

from 0% at the top of the cap to -3% at 250 km above the CMB (the bottom of the cap) and to -6% to the CMB. The high velocity region surrounding the low-velocity anomaly has a thickness of 250 km. From south to north, the high velocity structure has a velocity jump of 1.0 (2.0)% at 250 km above the CMB followed by a negative gradient from 1.0 (2.0)% to 0.0 (1.0)% and an aver-

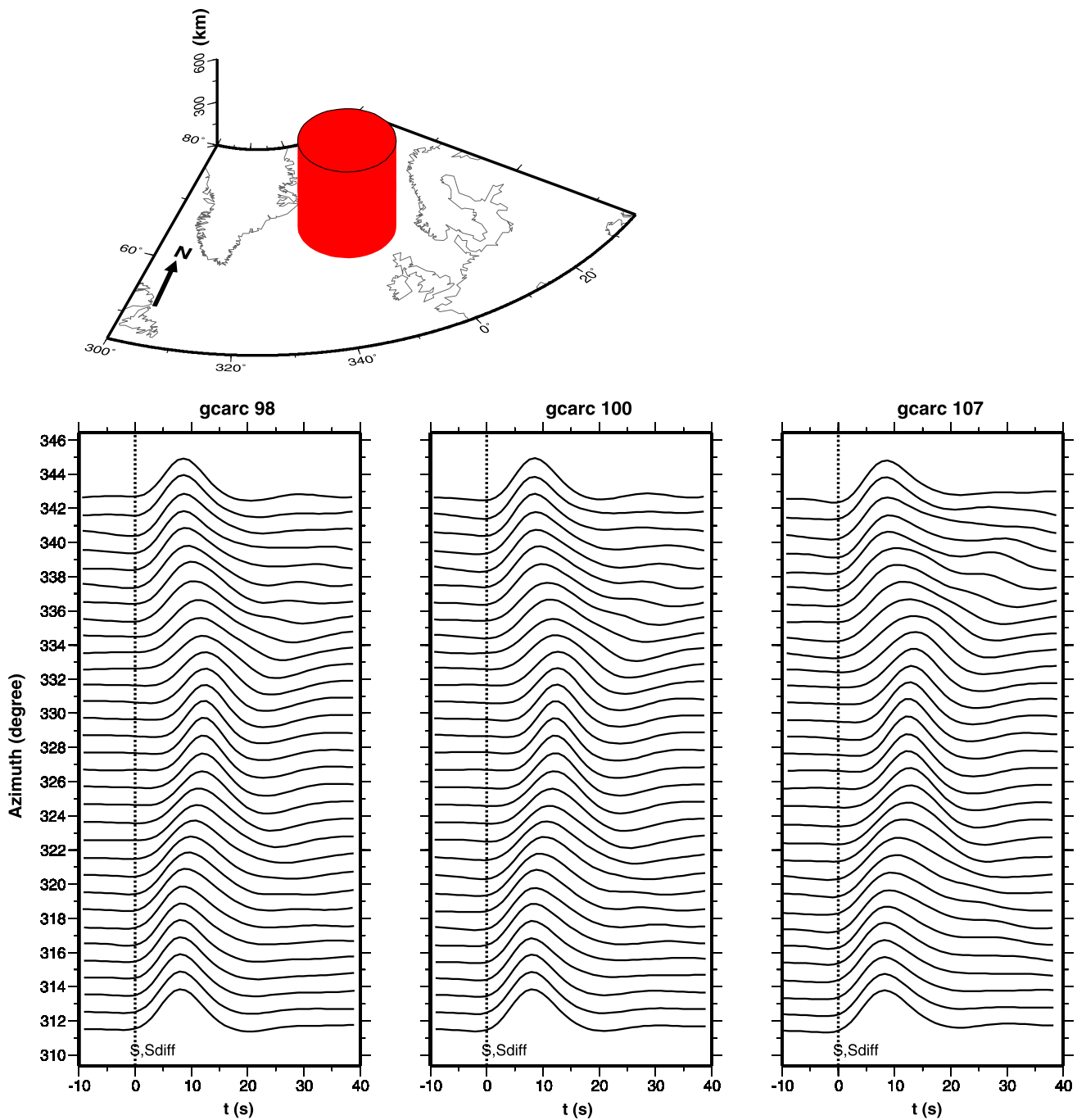


Fig. 4. Cylinder-shaped model and synthetics. Top panel: Cylinder-shaped model tested in our forward modeling process. It has a radius of 350 km and thickness of 600 km. The velocity structures vary from 0% at the top to -3% at 250 km above the CMB, and to -6% at the CMB. Bottom panel: Synthetics for event 2002/03/03 calculated based on the 3D model illustrated in the top model. We use the same hypocenter of event 2002/03/03 and theoretical stations with azimuths ranging from 312° to 343° . From left to right, the calculated displacements have different epicentral distances of 98° , 100° and 107° .

age shear-velocity reduction of -2.0% in the bottom 20 km of the mantle.

We further check the consistency of the best fitting mushroom-shaped model with the observed ScS–S and sScS–sS differential time residuals in the region (Figs. 1(b) and 6). We calculate synthetic seismograms for the preferred mushroom-shaped model for the ray paths shown in Fig. 1 using the 3-D waveform modeling method, and then hand-pick the ScS–S and sScS–sS differential time residuals from the synthetic seismograms. The travel time residuals from the synthetic seismograms of the preferred model exhibit positive values inside a circle with a 400-km radius cen-

tered beneath Iceland, and normal or negative values outside the circle, matching the geographic pattern of the observations (Figs. 6 and 1b). The maximum travel time residual (4.4 s) of the synthetics also fits the observed value well. However, we should point out that not all the observed travel time residuals outside the circle are explained by our model. For example, in the region north of the circle, the observed data exhibit positive travel time residuals while the synthetics predicts mostly negative values (cf., Figs. 1(b) and 6). Such discrepancy could be explained by existence of small-scale structure in the region or second-order geometric feature of the anomaly that is not accounted for by the idealized model pre-

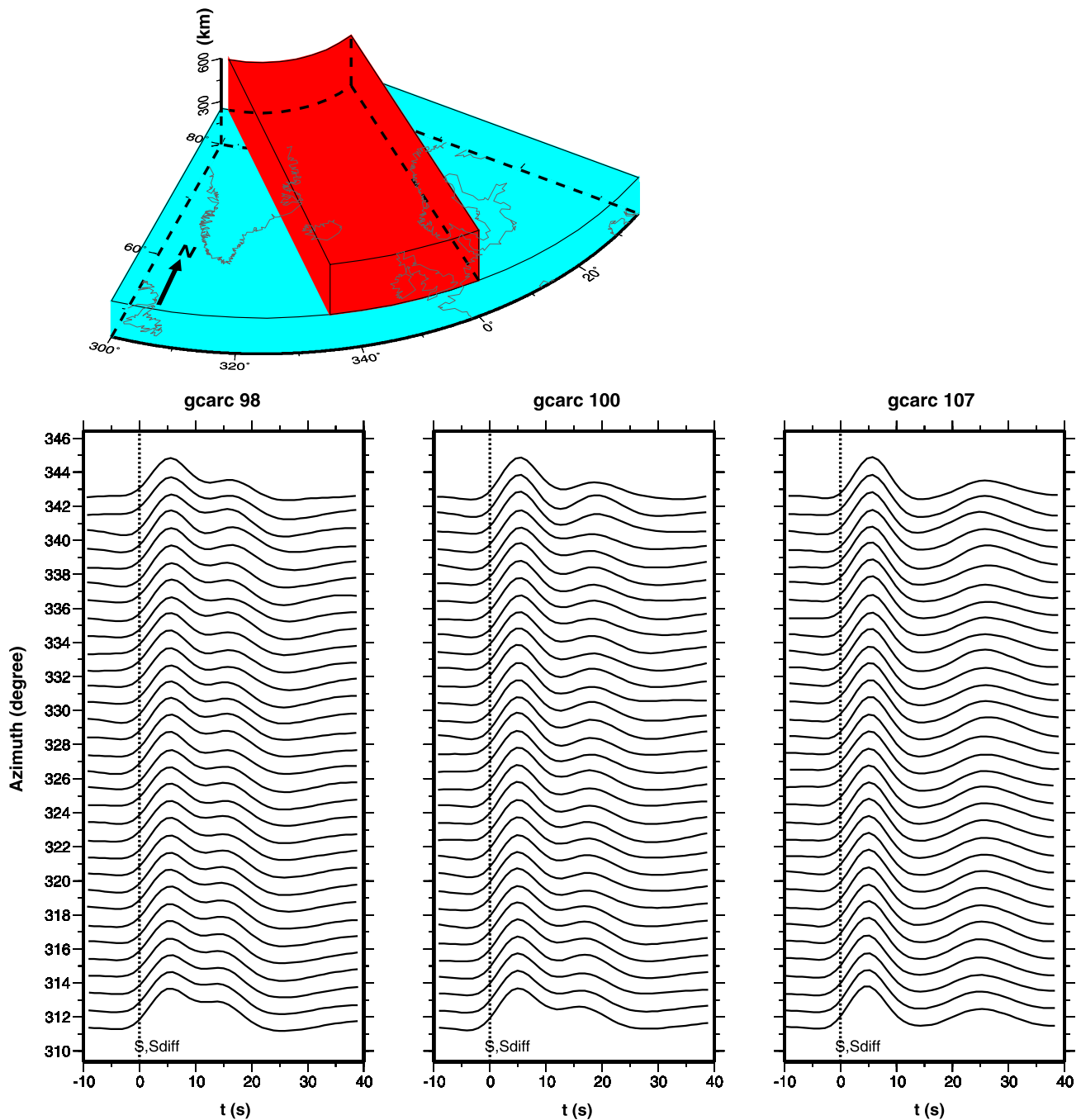


Fig. 5. Cuboid-shaped model and synthetics. Top panel: Cuboid-shaped model (red) overlies a high velocity structure (green). The cuboid-shaped model has a thickness of 350 km and a width of 1200 km. The length of the cuboid-model is long enough to produce a two-dimensional feature. The velocity structure varies from 0% at the top to -3% at the bottom of the cuboid-shaped model. The bottom high velocity structure has a thickness of 250 km and a velocity jump of 2.0% at 250 km above the CMB followed by a negative gradient from 2.0% to 0.0% and an average shear-velocity reduction of -2.0% in the bottom 20 km of the mantle. Bottom panel: Synthetics for event 2002/03/03 calculated based on the 3D model illustrated in the top model. From left to right, the calculated displacements have different epicentral distances of 98° , 100° and 107° . (For interpretation of the references to color in this figure legend, the reader is referred to the web version of this article.)

sented in the current study. Nevertheless, the synthetics of the preferred model match the first-order observations well, confirming the consistency of the best fitting mushroom-shaped model that was inferred from waveform modeling with the travel time data.

4. Thermal-chemical mantle plume as a possible explanation

The mushroom shape of the low-velocity anomaly and the model feature that the low-velocity anomaly is surrounded by a high-velocity structure with a D'' discontinuity (Fig. 3(a)) have

important implications to the dynamic process beneath Iceland. Mushroom shape is a typical morphology of a mantle plume in theoretical geodynamic modeling (Davies, 1999; Loper, 1991) and lab experiments (Griffiths and Campbell, 1990; Whitehead and Luther, 1975). Such shape suggests that Iceland represents a mantle plume developed in the lowermost mantle. If we interpret the surrounding high-velocity representative of downwelling in the lowermost mantle, the model feature of a low-velocity anomaly surrounded by a high-velocity structure further suggests two possible dynamic processes in developing Iceland plume: 1) convergence of downwelling to a local region at the CMB and the

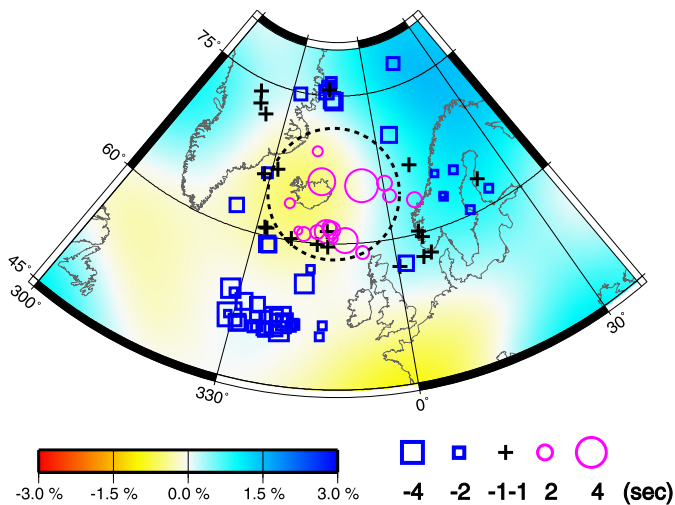


Fig. 6. Same as Fig. 1(b), except for synthetic ScS-S and sScS-sS differential time residuals of the preferred mushroom-shaped model inferred from waveform modeling. S, ScS, sS and sScS travel times are hand-picked from the synthetic seismograms generated based on the preferred model for the ray paths shown in Fig. 1 using a 3-D waveform modeling method (Capdeville et al., 2003).

thickening of the bottom thermal boundary layer developing an Iceland thermal plume (Tan et al., 2002), and 2) convergence of downwelling to a localized chemical anomaly generating an Iceland thermo-chemical plume. We favor the second scenario as the velocity reductions of the ultra low velocity zones (ULVZ) discovered at the base of the CMB beneath Iceland would require partial melting (Helmerger et al., 1998), making this portion of the lowermost mantle resembling more those of the African and Pacific Anomalies (Wen et al., 2001; He and Wen, 2009) than those of other low-velocity regions at the CMB. In another word, the observed ULVZ would favor a thermo-chemical origin of the Iceland root similar to the African and Pacific Anomalies. Considering the low-velocity anomalies discovered at various depths of the mantle beneath Iceland, from the shallow mantle (Tryggvason et al., 1983; Wolfe et al., 1997), the upper-mantle (Shen et al., 1998; Hung et al., 2004), the lower mantle (Bijwaard and Spakman, 1999; Montelli et al., 2006) to the lowermost mantle (Helmerger et al., 1998 and this study), we propose that Iceland represents a thermo-chemical plume generated by interaction of downwelling with a localized chemical anomaly at the base of the mantle. There is no active subduction near the Iceland since the breakup of Pangea (Wen and Anderson, 1995), but the downwelling could be associated with the subduction in the older tectonic history of the Earth.

Due to limited coverage of the seismic data, we have presented an idealized mushroom-shaped model in this study. When future data coverage is improved, further investigations on refined morphologic features and more detailed internal small-scale anomalies of the Iceland velocity structure would provide significant constraints on the origin and dynamic processes of the plume.

5. Conclusion

We utilize the observed ScS-S and sScS-sS differential travel-time residuals to constrain the geographic extent of the seismic anomaly near the CMB beneath Iceland. We further use 3-D waveform modeling of the seismic data sampling the lowermost mantle beneath Iceland to determine the detailed geometry and velocity structure of the Iceland anomaly in the lowermost mantle. Travel time analysis of ScS-S and sScS-sS phases exhibit a circular area of low velocities with radius of ~ 400 km beneath Iceland surrounded by normal or high-velocity regions. Waveform analysis suggests

that the Iceland low-velocity anomaly reaches at least 600 km above the CMB with a mushroom shape, and is surrounded by a high velocity province in the lowermost mantle. The inferred characteristics of the Iceland anomaly, in combination with the previous evidence of existence of ultra-low velocity zones at the base of the mantle beneath the region, suggest that Iceland represents a thermo-chemical plume generated by interaction of downwelling and a localized chemical anomaly at the base of the mantle.

Acknowledgements

We gratefully acknowledge the participants of the IRIS for its efforts in collecting the data. We thank Peter Shearer, Allen K. McNamara and one anonymous reviewer for comments and suggestions that improved the paper significantly. Figures were made with the General Mapping Tools (Wessel and Smith, 1995). This work was supported by the National Natural Science Foundation of China (grants 41474042 and 41125015) and Chinese Academy of Sciences and NSF grants 0911319 and 1214215.

Appendix A. Supplementary material

Supplementary material related to this article can be found online at <http://dx.doi.org/10.1016/j.epsl.2015.02.028>.

References

- Anderson, D.L., Natland, J.H., 2014. Mantle updrafts and mechanisms of oceanic volcanism. *Proc. Natl. Acad. Sci. USA* 111 (41), E4298–E4304. <http://dx.doi.org/10.1073/pnas.1410229111>.
- Bassin, C., Laske, G., Masters, G., 2000. The current limits of resolution for surface wave tomography in North America. *Eos Trans. AGU* 81 (48), Fall Meet. Suppl., Abstract S12A-03.
- Bijwaard, H., Spakman, W., 1999. Tomographic evidence for a narrow whole mantle plume below Iceland. *Earth Planet. Sci. Lett.* 166, 121–126.
- Capdeville, Y., To, A., Romanowicz, B., 2003. Coupling spectral elements and modes in a spherical Earth: an extension to the “sandwich” case. *Geophys. J. Int.* 154, 44–57.
- Davies, G.F., 1999. The Plume Mode. In: *Dynamic Earth: Plates, Plumes and Mantle Convection*. Cambridge University Press, Cambridge, pp. 293–323.
- Depaolo, D.J., Manga, M., 2003. Deep origin of hotspots – the mantle plume model. *Science* 300, 920–921.
- Dziewonski, A.M., Anderson, D.L., 1981. Preliminary reference Earth model. *Phys. Earth Planet. Inter.* 25, 297–356. [http://dx.doi.org/10.1016/0031-9201\(81\)90046-7](http://dx.doi.org/10.1016/0031-9201(81)90046-7).
- Dziewonski, A.M., Chou, T.A., Woodhouse, J.H., 1981. Determination of earthquake source parameters from waveform data for studies of global and regional seismicity. *J. Geophys. Res.* 86, 2825–2852. <http://dx.doi.org/10.1029/JB086iB04p02825>.
- Farley, K.A., Neroda, E., 1998. Noble gases in the Earth's mantle. *Annu. Rev. Earth Planet. Sci.* 26, 189–218.
- Foulger, G.R., 2002. Plumes, or plate tectonic processes? *Astron. Geophys.* 43, 6.19–6.23.
- Foulger, G.R., Du, Z., Julian, B.R., 2003. Icelandic-type crust. *Geophys. J. Int.* 155, 567–590.
- Grand, S.P., 2002. Mantle shear-wave tomography and the fate of subducted slabs. *Philos. Trans. R. Soc. Lond. A* 360, 2475–2491.
- Griffiths, R.E., Campbell, I.H., 1990. Stirring and structure in mantle starting plumes. *Earth Planet. Sci. Lett.* 99, 66–78.
- He, Y., Wen, L., 2009. Structural features and shear-velocity structure of the “Pacific Anomaly”. *J. Geophys. Res.* 114, B02309. <http://dx.doi.org/10.1029/2008JB005814>.
- Helmerger, D.V., Wen, L., Ding, X., 1998. Seismic evidence that the source of the Iceland hotspot lies at the core-mantle boundary. *Nature* 396, 251–255.
- Houser, C., Masters, G., Shearer, P., Laske, G., 2008. Shear and compressional velocity models of the mantle from cluster analysis of long-period waveforms. *Geophys. J. Int.* 174, 195–212. <http://dx.doi.org/10.1111/j.1365-246X.2008.03763.x>.
- Hung, S., Shen, Y., Chiao, L., 2004. Imaging seismic velocity structure beneath the Iceland hot spot: a finite frequency approach. *J. Geophys. Res.* 109, B08305. <http://dx.doi.org/10.1029/2003JB002889>.
- Kustowski, B., Ekström, G., Dziewoński, A.M., 2008. Anisotropic shear-wave velocity structure of the Earth's mantle: a global model. *J. Geophys. Res.* 113, B06306. <http://dx.doi.org/10.1029/2007JB005169>.
- Loper, D.E., 1991. Mantle plumes. *Tectonophysics* 187, 373–384.

- Montelli, R., Nolet, G., Dahlen, A., Masters, G.A., 2006. Catalogue of deep mantle plumes: new results from finite-frequency tomography. *Geochem. Geophys. Geosyst.* 7, Q11007. <http://dx.doi.org/10.1029/2006GC001248>.
- Morgan, J.W., 1971. Convection plumes in the lower mantle. *Nature* 230, 42–43.
- Mukhopadhyay, S., 2012. Early differentiation and volatile accretion recorded in deep-mantle neon and xenon. *Nature* 486, 101–104. <http://dx.doi.org/10.1038/nature11141>.
- Panning, M.P., Lekic, V., Romanowicz, B.A., 2010. The importance of crustal corrections in the development of a new global model of radial anisotropy. *J. Geophys. Res.* 115, B12325. <http://dx.doi.org/10.1029/2010JB007520>.
- Ritsema, J., van Heijst, H.J., Woodhouse, J.H., 1999. Complex shear wave velocity structure imaged beneath Africa and Iceland. *Science* 286, 1925–1928.
- Ritsema, J., Duess, A., van Heijst, H.J., Woodhouse, J.H., 2011. S40RTS: a degree–40 shear-velocity model for the mantle from new Rayleigh wave dispersion, teleseismic traveltimes and normal-mode splitting function measurements. *Geophys. J. Int.* 184, 1223–1236. <http://dx.doi.org/10.1111/j.1365-246X.2010.04884.x>.
- Shen, Y., Solomon, S.C., Bjarnason, I.Th., Wolfe, C.J., 1998. Seismic evidence for a lower-mantle origin of the Iceland plume. *Nature* 395, 62–65.
- Simmons, N.A., Forte, A.M., Boschi, L., Grand, S.P., 2010. GyPSuM: a joint tomographic model of mantle density and seismic wave speeds. *J. Geophys. Res.* 115, B12310. <http://dx.doi.org/10.1029/2010JB007631>.
- Tan, E., Gurnis, M., Han, L., 2002. Slabs in the lower mantle and their modulation of plume formation. *Geochem. Geophys. Geosyst.* 3, 1067. <http://dx.doi.org/10.1029/2001GC000238>.
- Tryggvason, K., Husebye, E.S., Stefánsson, R., 1983. Seismic image of the hypothesized Icelandic hot spot. *Tectonophysics* 100, 97–118.
- Wen, L., Anderson, D.L., 1995. The fate of slabs inferred from seismic tomography and 130 million years of subduction. *Earth Planet. Sci. Lett.* 133, 185–198.
- Wen, L., Silver, P., James, D., Kuehnel, R., 2001. Seismic evidence for a thermochemical boundary at the base of the Earth's mantle. *Earth Planet. Sci. Lett.* 189, 141–153.
- Wessel, P., Smith, W.H.F., 1995. New version of the Generic Mapping Tools released. *Eos Trans. AGU* 76 (33), 329.
- Whitehead, J.A., Luther, D.S., 1975. Dynamics of laboratory diapir and plume models. *J. Geophys. Res.* 80, 705–717.
- Wolfe, C.J., Bjarnason, I.Th., VanDecar, J.C., Solomon, S.C., 1997. Seismic structure of the Iceland mantle plume. *Nature* 385, 245–247.
- Zhao, D., 2001. Seismic structure and origin of hotspots and mantle plumes. *Earth Planet. Sci. Lett.* 192, 251–265.